

See discussions, stats, and author profiles for this publication at: <https://www.researchgate.net/publication/231664028>

# Analysis of Spatial Contribution to the Second Hyperpolarizabilities of $\pi$ -Conjugated Systems Involving Sulfur Atoms

ARTICLE *in* THE JOURNAL OF PHYSICAL CHEMISTRY A · MARCH 1999

Impact Factor: 2.69 · DOI: 10.1021/jp984665n

---

CITATIONS

28

---

READS

21

3 AUTHORS, INCLUDING:



Masayoshi Nakano

Osaka University

337 PUBLICATIONS 4,769 CITATIONS

SEE PROFILE

# Analysis of Spatial Contribution to the Second Hyperpolarizabilities of $\pi$ -Conjugated Systems Involving Sulfur Atoms

Masayoshi Nakano,\* Satoru Yamada, and Kizashi Yamaguchi

Department of Chemistry, Graduate School of Science, Osaka University, Toyonaka, Osaka 560-0093, Japan

Received: December 8, 1998

We study the third-order optical nonlinearity for some interesting  $\pi$ -conjugated systems involving sulfur (S) atoms. First, we investigate the static second hyperpolarizabilities ( $\gamma$ ) for 1,6,6a-trithiapentalene (TTP) and its donor (D)- and acceptor (A)-disubstituted model species by using ab initio molecular orbital and density functional methods. By using the second hyperpolarizability density analysis, which can elucidate spatial contributions of electrons to  $\gamma$ , these molecules are found to exhibit interesting differences in contributions of unusual binding structure, i.e., S–S–S bridged structure, to the longitudinal  $\gamma$ . Secondly, we investigate the static  $\gamma$  for another  $\pi$  conjugated system involving sulfur atoms, i.e., cation radical state of tetrathiafulvalene (TTF). This molecule is found to provide unique third-order optical nonlinearity, i.e., large negative  $\gamma$ . We finally discuss a possibility of multiproperty aggregate systems combining the unique third-order optical nonlinearity and high electrical conductivity.

## 1. Introduction

Many experimental and theoretical studies on the third-order optical nonlinearity for organic systems have been performed in order to explore the relations among nonlinear optical response properties and electronic structures and to design novel third-order nonlinear optical materials.<sup>1,2</sup> In previous papers,<sup>3,4</sup> we investigated a structure-property correlation rule for second hyperpolarizability ( $\gamma$ ), which can describe molecular third-order nonlinear optical polarization. It was found that  $\gamma$  is considered to be a measure of third-order electron fluctuation and that  $\gamma$  is remarkably affected by slight changes in the electronic structure. In this study, as a new class of third-order nonlinear optical systems, we consider some  $\pi$ -conjugated systems involving sulfur (S) atoms with unique binding and electronic structures.

Firstly, the  $\gamma$  value of 1,6,6a-trithiapentalene (TTP) shown in Figure 1a (X = H) is investigated. Its electronic and molecular structures have been investigated experimentally and theoretically for many years because of the unusual three-coordinated structure around the S atoms.<sup>5–10</sup> There were two types of structures proposed as shown in Figures 1b and 1c. The resonance structure shown in Figure 1b indicates the “single-bond no-bond resonance”, corresponding to the symmetrical  $C_{2v}$  structure, while the structure shown in Figure 1c is interpreted by valence tautomerization between the two alternate forms, which are asymmetric structures. In this case, the  $C_{2v}$  form represents a transition state. For the structure shown in Figure 1b, the energy potential has a single minimum, while for the structure shown in Figure 1c, the energy potential has a double minimum. If the energy barrier is too low to be observed by the experimental methods used, distinctions between real (Figure 1b) or time-averaged (Figure 1c)  $C_{2v}$  symmetry may be impossible. Recent experimental and theoretical studies elucidated that TTP can be a  $C_{2v}$  symmetrical equilibrium structure with a unique linear arrangement of three-center S atoms.<sup>6,8</sup> It was also found that ab initio Hartree–Fock (HF) method with large-size basis sets can predict incorrect equilibrium structures, which are asymmetric forms, while the electron correlation

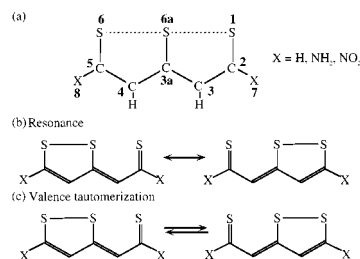


**Figure 1.** (a) Labeling of the atoms in 1,6,6a-trithiapentalene (TTP (X = H)) and disubstituted TTP (X = NH<sub>2</sub> and NO<sub>2</sub>). (b) Single-bond no-bond resonance structures. (c) Valence tautomerization between the two alternate forms.

methods, e.g., Møller–Plesset second-order perturbation (MP2), MP4, and density functional (DF) methods can provide  $C_{2v}$  symmetric structures in the ground state.<sup>6,8–10</sup> Namely, the ground-state potential is concluded to be a very flat U-shaped function with a single minimum. Therefore, the unique electronic structure of TTP is expected to provide interesting features of its longitudinal  $\gamma$ . In this study, the spatial contributions of electrons to the longitudinal  $\gamma$  are elucidated by using the plots of second hyperpolarizability density<sup>11</sup> calculated by ab initio MP2 and DF methods using standard and extended basis sets.

Secondly, we examine the longitudinal  $\gamma$  for donor (D)- and acceptor (A)-disubstituted TTP models shown in Figure 1a (X = NH<sub>2</sub> and NO<sub>2</sub>). Considering the very flat U-shaped energy curve and unique S–S–S binding for TTP, the ground-state electronic states are expected to be sensitively influenced by minute chemical perturbation, e.g., the introduction of D and A groups into the 2 and 5 positions (See Figure 1a). We consider two model systems which are respectively disubstituted by D(=NH<sub>2</sub>) and A(=NO<sub>2</sub>) groups (See Figure 1a, X = NH<sub>2</sub> and NO<sub>2</sub>). The  $\gamma$  values and their densities are calculated by DF method using extended basis sets. Since these substituent groups are considered to largely affect the  $\pi$ -electron distribution on S–S–S sites, the  $\gamma$  values for these systems are expected to be significantly different from that for unsubstituted TTP.

The sign of  $\gamma$  is important in quantum optics:<sup>12</sup> the positive value causes the self-focusing effect of an incident beam, while the negative one does the self-defocusing effects. Further, it is interesting to investigate the nonlinear optical systems with negative large  $\gamma$  since such systems are rare in general and the signs and magnitudes of  $\gamma$  are exceptionally sensitive to subtle changes of the structures.<sup>4,13,14</sup> Namely, these systems are also expected to be a candidate for fundamental systems of “controllable nonlinear optical materials”.<sup>4</sup> On the basis of our structure-property correlation rule for  $\gamma$ , systems which have large contribution of symmetric resonance structures with inversible polarization (SRIP)<sup>4</sup> are expected to exhibit negative  $\gamma$ . As models with negative  $\gamma$ , we have proposed anion radical condensed-ring conjugated systems<sup>3,13</sup> and nitronyl nitroxide radical systems.<sup>15,16</sup> Their  $\gamma$  values were predicted to be negative in sign by using high-order electron correlation methods starting from coupled Hartree–Fock (CHF) results.<sup>4,16</sup>

Finally, therefore, as a novel model system with negative  $\gamma$ , we consider an alternant  $\pi$ -conjugated system involving S atoms, i.e., the cation radical state of tetrathiafulvalene (TTF<sup>+</sup>) shown in Figure 2d. From our recent study,<sup>17</sup> longitudinal  $\gamma$  for TTF<sup>+</sup> calculated by DF method using extended basis sets was found to be negative in sign. This system is also considered to be element molecules constructing various types of molecular aggregates including high electrical conductive molecular aggregates.<sup>18</sup> In this study, therefore, we predict the features of  $\gamma$  for segregated molecular aggregates based on the calculation result of TTF<sup>+</sup>, and also discuss a possibility of multiproperty aggregate systems combining unique optical nonlinearity and high electrical conductivity, from the viewpoint of our structure-property correlation rule for unique third-order nonlinear optical systems.

The present paper is organized as follows. In section 2, we explain our structure-property correlation rule for  $\gamma$ . In section 3, we explain the calculation and analysis methods and show molecular geometries of model systems. The results of TTP and D (A)-disubstituted TTP are discussed in sections 4 and 5, respectively. In section 6, the results of TTF<sup>+</sup> and a prediction of features of  $\gamma$  for a segregated aggregate model are presented. A possibility of multiproperty aggregate systems combining unique optical nonlinearity and high electrical conductivity is also discussed. This is followed by a conclusion in section 7.

## 2. Structure-Property Correlation Rule for Third-order Nonlinear Optical Systems

We here briefly explain our structure-property correlation rule for molecular systems. The perturbative formula for  $\gamma$  can be partitioned into three types of contributions (I, II, and III) as follows:<sup>3</sup>

$$\gamma^{\text{I} + \text{II} + \text{III}} = \gamma^{\text{I}} + \gamma^{\text{II}} + \gamma^{\text{III}} \quad (1)$$

where

$$\gamma^{\text{I}} = \sum_{n=1} \frac{(\mu_{n0})^2 (\mu_{nn})^2}{E_{n0}^3} \quad (2)$$

$$\gamma^{\text{II}} = - \sum_{n=1} \frac{(\mu_{n0})^4}{E_{n0}^3} \quad (3)$$

and

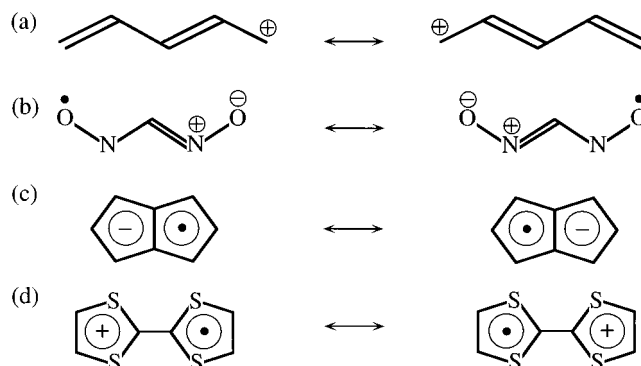


**Figure 2.** Symmetric resonance structures with inversible polarization (SRIP) for various  $\pi$ -conjugated systems, i.e., (a) charged soliton-like oligomer, (b) nitronyl nitroxide radical, (c) anion radical state of pentalene, and (d) cation radical state of tetrathiafulvalene (TTF<sup>+</sup>).

$$\gamma^{\text{III}} = \sum_{\substack{m,n=1 \\ (m \neq n)}} \frac{(\mu_{n0})^2 (\mu_{mn})^2}{E_{n0}^2 E_{m0}} \quad (4)$$

Here,  $\mu_{n0}$  is the transition moment between the ground and the  $n$ th excited states,  $\mu_{mn}$  is the transition moment between the  $m$ th and the  $n$ th excited states,  $\mu_{nn}$  is the difference of dipole moments between the ground and the  $n$ th excited states and  $E_{n0}$  is the transition energy given by  $(E_n - E_0)$ . From these equations, apparently, the contributions of types I and III are positive in sign, whereas the contribution of type II is negative. For conventional molecular compounds with large positive  $\gamma$ , there are two characteristic cases: i)  $|\gamma^{\text{I}}| \gg |\gamma^{\text{II}}| \approx |\gamma^{\text{III}}|$  ( $\gamma > 0$ ) and ii)  $|\gamma^{\text{I}}| = 0$ ,  $|\gamma^{\text{II}}| < |\gamma^{\text{III}}|$  ( $\gamma > 0$ ). In the case i, the compounds have large nonsymmetric charge distributions which are responsible for large  $\mu_{nn}$ , whereas in the case ii, the compounds are centrosymmetric systems in which the contributions of type I disappear. The third case, i.e., iii)  $|\gamma^{\text{I}}| = 0$ ,  $|\gamma^{\text{II}}| > |\gamma^{\text{III}}|$  ( $\gamma < 0$ ), is interesting because the systems with negative static  $\gamma$  is rare in general. Such systems are symmetric ( $\mu_{nn} = 0$ ) and exhibit strong virtual excitation between the ground and the first excited states ( $|\mu_{0n}| > |\mu_{nn}|$ ). This indicates that the symmetric systems with large ground-state polarizability ( $\alpha_0$ ) tend to exhibit negative  $\gamma$ . Figure 2 shows resonance structures mainly contributing to the ground state of  $\pi$  conjugated systems with large  $\alpha_0$ , i.e., (a) charged soliton-like oligomer, (b) nitronyl nitroxide radical, (c) anion radical state of pentalene, and (d) TTF<sup>+</sup>. These indicate the resonances between polarized structures with mutually opposite directions, and they can significantly contribute to the stability of ground-state electronic structures. The large contribution of these resonance structures also correspond to the fact that the magnitude of transition moment ( $\mu_{n0}$ ) between the ground and the first excited states are large. As seen from the previous results for systems (shown in Figure 2a–c),<sup>2,4,16</sup> a system with resonance structures contributing to the stability of the ground state and inducing the polarization in the mutually opposite direction tends to exhibit negative  $\gamma$  and remarkable electronic structure dependences of the  $\gamma$ . The large contribution of the stable resonance structures with large dipole moments corresponds to an enhancement of the magnitude of the transition moment ( $\mu_{n0}$ ) between the ground and the allowed first excited states. This contribution also leads to a reduction of the transition energy ( $E_{n0}$ ) between the ground and the allowed first excited states with large contributions from the resonance structures. As a result, a system with large contribution of symmetric resonance structures with inversible polarization, i.e., SRIP, satisfies our criteria for the system to have a negative  $\gamma$ .

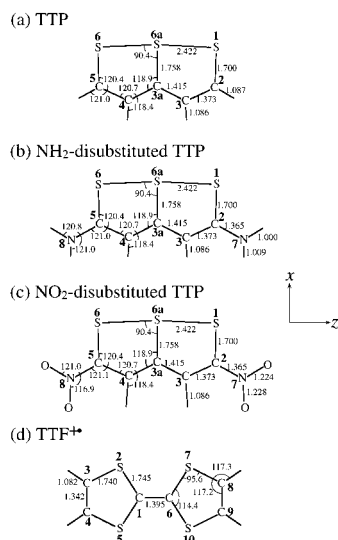


**Figure 3.** Bond distances [Å] and bond angles [deg] of (a) 1,6,6a-trithiapentalene (TTP), (b) donor(NH<sub>2</sub>)-disubstituted TTP, (c) acceptor(NO<sub>2</sub>)-disubstituted TTP, and (d) cation radical tetrathiafulvalene (TTF<sup>•+</sup>). The structure of TTP (a) is optimized by B3LYP method with 6-311G<sup>••</sup>. For the disubstituted TTP (b and c), only the structures of NH<sub>2</sub> and NO<sub>2</sub> groups are optimized by B3LYP method with 6-31G<sup>\*</sup> using the fixed TTP structure a. The structure of TTF<sup>•+</sup> is optimized by B3LYP method with 6-311G<sup>••</sup>. The numbers labeled on atoms are also shown.

### 3. Calculation Methods, Calculated Molecules, and Analysis Method

**3.1. Calculation Methods and Calculated Molecules.** Figure 3 shows molecular geometries for (a) TTP, (b) D(=NH<sub>2</sub>)-disubstituted TTP, (c) A(=NO<sub>2</sub>)-disubstituted TTP and (d) TTF<sup>•+</sup>. It was found that TTP optimized by MP2, MP4, and DF (B3LYP<sup>19</sup>) methods possess planar structures with C<sub>2v</sub> symmetry and their structure parameters are in good agreement with experimental data<sup>6,7</sup> though the structure optimization by HF method provides incorrect asymmetric structures. Therefore, we optimize the geometries of TTP under the constraint of planar structures with C<sub>2v</sub> symmetry by using B3LYP method with 6-31G<sup>••</sup> basis set. In this study, we confine our attention to the qualitative effects of the introduction of D and A groups to the  $\gamma$  and its density distribution. Therefore, we consider D(A)-disubstituted TTP models (See Figures 3b and 3c), in which only the structures of D and A groups are optimized by using B3LYP method with 6-31G<sup>\*</sup> basis set, and the structure of TTP skeleton is fixed to that of unsubstituted TTP shown in Figure 3a. The geometries of TTF<sup>•+</sup> are optimized by using B3LYP with 6-311G<sup>••</sup>. All calculations are performed by using GAUSSIAN94 program package.<sup>20</sup>

It is well-known that extended basis sets augmented by diffuse and polarization functions (p and d) are at least necessary for reproducing qualitative  $\gamma$  for hydrocarbon compounds. In the previous papers,<sup>4,13</sup> we investigated the basis set dependences of  $\gamma$  for three charged state pentalenes (neutral, anion radical, and dianion states) by using the standard (split-valence (6-31G)) and extended basis sets augmented by diffuse and polarization functions (6-31G+pd ( $\zeta_{p,d}$  = 0.0523 for carbon (C) atoms) and 6-31G+d ( $\zeta_d$  = 0.0523 for carbon (C) atoms). The exponents of these functions ( $\zeta_{p,d}$  and  $\zeta_d$ ) were determined from the outermost two exponents of 6-31G by the even tempered method. It is found from this investigation that the calculations using 6-31G+d basis set can reproduce at least longitudinal components of  $\gamma$  for pentalene calculated by using 6-31G+pd

basis set. In this study, we use 6-31G<sup>•</sup>+pd ( $\zeta_{p,d}$  = 0.0523 for C atoms,  $\zeta_{p,d}$  = 0.0402 for S atoms, and  $\zeta_{p,d}$  = 0.0719 for O atoms) and 6-31G<sup>\*</sup> basis sets in order to elucidate the basis set dependence of  $\gamma$  for TTP. The relatively compact basis sets, i.e., 6-31G<sup>•</sup>+d and 6-31G<sup>••</sup>+d ( $\zeta_{p,d}$  = 0.0523 for C atoms,  $\zeta_{p,d}$  = 0.0402 for S atoms,  $\zeta_{p,d}$  = 0.0582 for nitrogen (N) atoms, and  $\zeta_{p,d}$  = 0.0719 for O atoms), are used for disubstituted TTP and TTF<sup>•+</sup>, respectively, to avoid large-scale calculations. Judging from our results for pentalene, these basis sets are predicted to well reproduce the  $\gamma$  values for these systems calculated by using 6-31G+pd and 6-31G<sup>••</sup>+pd. A DF method, i.e., B3LYP method, is applied to the calculations of  $\gamma$  since electron correlation effects on  $\gamma$  are known to be well reproduced by B3LYP method.<sup>21</sup> For TTP, an ab initio electron correlation method, i.e., MP2 method, is also used in order to compare the electron correlation effects considered by MP2 method with those considered by B3LYP method. We confine our attention to the longitudinal components  $\gamma_{zzzz}$  ( $\gamma$ ), which are main components for systems considered in this study.

In finite-field (FF) approach, the  $\gamma$  is calculated by a numerical differentiation of the total energy  $E$  with respect to the applied field by

$$\gamma_{zzzz} = \{E(3F^z) - 12E(2F^z) + 39E(F^z) - 56E(0) + 39E(-F^z) - 12E(-2F^z) + E(-3F^z)\}/36(F^z)^4 \quad (5)$$

Here,  $E(F^z)$  indicates the total energy in the presence of the field  $F^z$  applied in the  $z$  direction. In order to avoid numerical errors, we use several minimum fields strengths. After numerical differentiations using these fields, we adopt a numerically stable  $\gamma$ , which is found to be obtained by using fields, 0.002 au, for these systems.

**3.2. Hyperpolarizability Density Analysis.** We explain hyperpolarizability density analysis of the static  $\gamma$  in FF approach. The charge density function  $\rho(\mathbf{r}, \mathbf{F})$  can be expanded in powers of the field  $\mathbf{F}$  as

$$\rho(\mathbf{r}, \mathbf{F}) = \rho^{(0)}(\mathbf{r}) + \sum_j \rho_j^{(1)}(\mathbf{r}) F_j + \frac{1}{2!} \sum_{jk} \rho_{jk}^{(2)}(\mathbf{r}) F_j F_k + \frac{1}{3!} \sum_{jkl} \rho_{jkl}^{(3)}(\mathbf{r}) F_j F_k F_l + \dots \quad (6)$$

From this equation and the following expansion formula of dipole moment in powers of the field:

$$\mu^i(\mathbf{F}) = - \int \mathbf{r}^i \rho(\mathbf{r}, \mathbf{F}) d\mathbf{r}^3 = \mu_0^i + \sum_j \alpha_{ij} F_j + \sum_{jk} \beta_{ijk} F_j F_k + \sum_{jkl} \gamma_{ijkl} F_j F_k F_l + \dots \quad (7)$$

the static  $\gamma$  can be expressed by

$$\gamma_{ijkl} = - \frac{1}{3!} \int \mathbf{r}^i \rho_{jkl}^{(3)}(\mathbf{r}) d\mathbf{r}^3 \quad (8)$$

where

$$\rho_{jkl}^{(3)}(\mathbf{r}) = \left. \frac{\partial^3 \rho}{\partial F^j \partial F^k \partial F^l} \right|_{\mathbf{F}=0} \quad (9)$$

This third-order derivative of the electron density with respect to the applied electric fields is referred to as the second hyperpolarizability ( $\gamma$ ) density. In this study, we confine our attention to the  $\gamma$  density ( $\rho_{zzz}^{(3)}(\mathbf{r})$ ) which are calculated at each



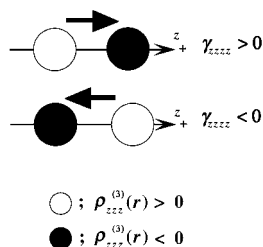


**Figure 4.** Schematic diagram of the second hyperpolarizability ( $\gamma_{zzzz}$ ) densities  $\rho_{zzz}^{(3)}(\mathbf{r})$ . The size of circle represents the magnitude of  $\rho_{zzz}^{(3)}(\mathbf{r})$ , and the arrow shows the sign of  $\gamma_{zzzz}$  determined by the relative spatial configuration between these two  $\rho_{zzz}^{(3)}(\mathbf{r})$ .

spatial point in the discretized space by using the following third-order numerical differentiation formula.

$$\rho_{zzz}^{(3)}(\mathbf{r}) = \frac{\{\rho(\mathbf{r}, 2F^z) - \rho(\mathbf{r}, -2F^z) - 2(\rho(\mathbf{r}, F^z) - \rho(\mathbf{r}, -F^z))\}}{2(F^z)^3} \quad (10)$$

where  $\rho(\mathbf{r}, F^z)$  represents the charge density at a spatial point  $\mathbf{r}$  in the presence of the field  $F^z$ . The charge densities over a three-dimensional grid of points are evaluated by the density matrix obtained by GAUSSIAN 94 program package.

In order to explain the analysis procedure by using the  $\gamma$  densities ( $\rho_{zzz}^{(3)}(\mathbf{r})$ ), let us consider a pair of localized  $\rho_{zzz}^{(3)}(\mathbf{r})$  shown in Figure 4. The positive sign of the  $\rho_{zzz}^{(3)}(\mathbf{r})$  implies that the second derivative of the charge density increases with the increase in the field. The arrow from a positive to a negative  $\rho_{zzz}^{(3)}(\mathbf{r})$  shows the sign of the contribution determined by the relative spatial configuration between the two  $\rho_{zzz}^{(3)}(\mathbf{r})$ . Namely, the sign of the contribution becomes positive when the direction of the arrow coincides with the positive direction of the coordinate system. The contribution determined by the  $\rho_{zzz}^{(3)}(\mathbf{r})$  of the two points is more significant, when their distance is larger.

#### 4. $\gamma$ and $\gamma$ Densities for TTP

Figure 5 shows  $\gamma$  values and  $\gamma$  density plots for TTP (shown in Figure 3a) calculated by B3LYP and ab initio MP2 methods using 6-31G\* and 6-31G\*+pd basis sets. Since it is well-known that  $\pi$ -electrons dominantly contribute to the  $\gamma$  for  $\pi$ -conjugated

systems, we consider the  $\gamma$  density distributions on the plane located at 2 au above the molecular plane.

**4.1. Comparison between B3LYP and MP2 Results.** As shown in Figure 5, the qualitative features of  $\gamma$  values and  $\gamma$  density distributions calculated by B3LYP method are similar to those by MP2 method. This supports our previous results,<sup>22</sup> in which B3LYP method is shown to reproduce the  $\gamma$  values and  $\gamma$  density distributions calculated by high-order electron correlation methods, e.g., MP4 and quadratic configuration interaction involving single and double excitations (QCISD) methods. To better investigate the electron correlation effects involved in B3LYP results, we should obtain the  $\gamma$  values and  $\gamma$  density plots calculated by higher-order electron correlation methods, e.g., MP4 and QCISD methods using extended basis sets, which are difficult to be performed for these large-size systems anywhere due to the lack of computer resources at the present time. In this study, therefore, we use the  $\gamma$  values and  $\gamma$  density plots calculated by B3LYP method in the following discussion.

**4.2. Basis Set Dependency of  $\gamma$ .** First, we consider a partition of the  $\gamma$  density distributions for the system into two spatial regions, respectively involving S—S—S and H—C—CH—C—CH—C—H units. This partition is described by dotted lines shown in Figures 5a and b. We also calculate the  $\gamma$  values for these two regions. These  $\gamma$  values are considered to reflect the qualitative features of  $\pi$ -electron contributions from these two units, i.e., S—S—S and H—C—CH—C—CH—C—H, though the  $\gamma$  values are calculated only at a plane located at 2 au above the molecular plane.

The basis set dependence is found to be remarkable. As changing the basis set from 6-31G\* to 6-31G\*+pd, the sign of  $\gamma$  is changed from negative to positive and its magnitude is about 8 times enhanced (see Figures 5a and b). It is found from the  $\gamma$  density plots (Figures 5a and b) that the main contribution to the  $\gamma$  originates in the S—S—S region, which provides negative (at 6-31G\*) and positive (at 6-31G\*+pd) contributions. This change in sign is caused by the appearance of  $\gamma$  densities with large positive contributions in the outer regions. Namely, the augmentation of diffuse (p and d) functions are considered to be necessary for the qualitatively adequate description of  $\pi$  electron contribution in the S—S—S region. In contrast, in H—C—CH—C—CH—C—H region, there is no remarkable appearance of  $\gamma$  densities in the outer region and considerable cancellation among positive and negative  $\gamma$  contributions occurs

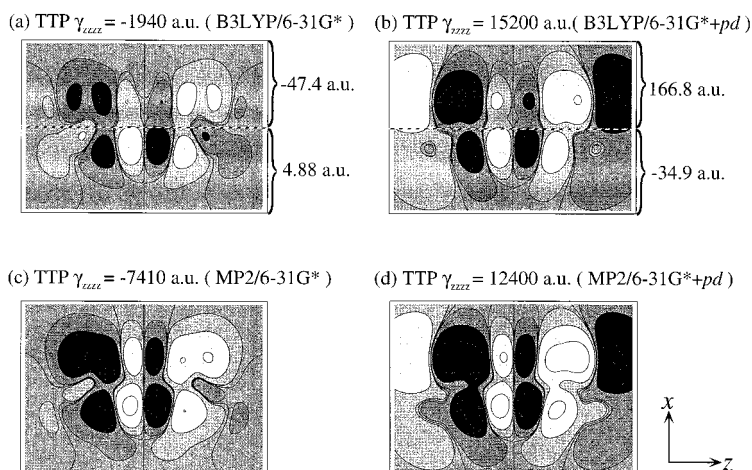


**Figure 5.** Calculated  $\gamma_{zzzz}$  values and plots of  $\gamma_{zzzz}$  densities on the planes located at 2 au above the molecular planes of 1,6,6a-trithiapentalene (TTP) (shown in Figure 3a). The B3LYP (a and b) and MP2 (c and d) results are shown for a standard (6-31G\*) and an extended (6-31G\*+pd) basis sets. The  $\gamma_{zzzz}$  values in two regions (partitioned by dotted lines), i.e., S—S—S and H—C—CH—C—CH—C—H regions for B3LYP results are also shown in the right hand-side of each plot. Contours are drawn at 50, 10, 1, 0, -1, -10, and -50 au.

## Mulliken charge density for TTP

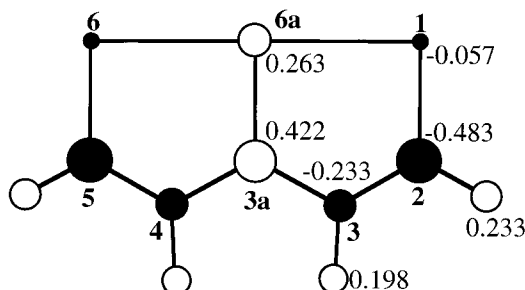


**Figure 6.** Mulliken charge density plots for 1,6,6a-trithiapentalene (TTP) (Figure 3a) calculated by B3LYP/6-31G\*+pd method. The positive and black circles represent positive and negative charges, respectively.

though the augmentation of basis set is found to reverse the sign of the partitioned  $\gamma$  in H-C-CH-C-CH-C-H region.

**4.3. Feature of  $\gamma$  Density Distribution.** Judging from our structure-property correlation rule using SRIP and the main resonance structure shown in Figure 1b, the  $\gamma$  of TTP is predicted to be positive in sign. In fact, the  $\gamma$  value for TTP calculated by B3LYP/6-31G\*+pd is found to be positive in sign. It is found from Figure 5b that the main contribution to  $\gamma$  for TTP originates in the S-S-S region. It is also found that the  $\pi$ -electron contribution to  $\gamma$  in the H-C-CH-C-CH-C-H region of TTP is negative, while that in the S-S-S region is positive.

In order to estimate the features of SRIP contributions for TTP, we investigate the Mulliken charge density distributions of TTP (see Figure 6). It is found that S atom at **6a** is positively charged (0.263), while the other S atoms at **1** and **6** are slightly negatively charged (-0.057). On the other hand, the H-C-CH-C-CH-C-H region is found to exhibit a remarkable positive-negative charge separation: the central C atom at **3a** is positively charged (0.422), while the both-side C atoms at **2**, **3**, **4**, and **5** are negatively charged (-0.233 (**3** and **4**) and -0.483 (**2** and **5**)). From such feature of charge distributions, it is presumed that in the S-S-S region of TTP, small SRIP contribution and large  $3p\pi$  electron contributions lead to the large positive partitioned  $\gamma$  (166.8 au on the plane shown in Figure 5b), while in the H-C-CH-C-CH-C-H region of TTP, relatively large SRIP contribution due to the positive-negative charge separation causes negative partitioned  $\gamma$  (-34.9 au on the plane shown in Figure 5b). It is noted that the feature of  $\gamma$  density distribution in the H-C-CH-C-CH-C-H region of TTP is similar to that of charged soliton-like oligomers which are found to exhibit negative  $\gamma$ .<sup>11,23</sup>

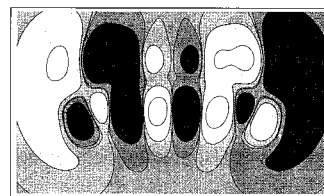
## 5. $\gamma$ and $\gamma$ Densities for D- and A-Disubstituted TTP

Figure 7 shows  $\gamma$  values and  $\gamma$  density plots for D(=NH<sub>2</sub>)- and A(=NO<sub>2</sub>)-disubstituted TTP (shown in Figure 3b and c) calculated by B3LYP method using 6-31G\*+d basis set. Similarly to the TTP case, we consider the  $\gamma$  density distributions on the plane located at 2 au above the molecular plane.

Both disubstituted TTP are found to exhibit about two times larger  $\gamma$  values than TTP. However, these enhancements of  $\gamma$  are not considered to be caused only by the contributions of the substituent groups (NH<sub>2</sub> and NO<sub>2</sub>).

For NH<sub>2</sub>-disubstituted TTP (Figure 7a), the  $\gamma$  densities in the S-S-S region, which contributes to  $\gamma$  positively, are remarkably enhanced compared with those for TTP (see Figure 5b).

(a) NH<sub>2</sub>-disubstituted TTP  $\gamma_{zzzz} = 28700$  a.u. (B3LYP/6-31G\*+d)



(b) NO<sub>2</sub>-disubstituted TTP  $\gamma_{zzzz} = 33500$  a.u. (B3LYP/6-31G\*+d)

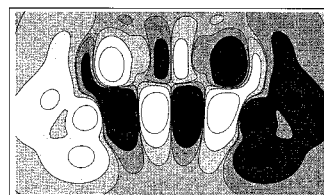


**Figure 7.** Calculated  $\gamma_{zzzz}$  values and plot of  $\gamma_{zzzz}$  densities on the plane located at 2 au above the molecular planes of (a) NH<sub>2</sub>- and (b) NO<sub>2</sub>-disubstituted trithiapentalene (TTP). The B3LYP method using an extended (6-31G\*+d) basis set is used. Contours are drawn at 50, 10, 1, 0, -1, -10, and -50 au.

TTF<sup>•+</sup>  $\gamma_{zzzz} = -5200$  a.u. (B3LYP/6-31G\*\*+d)

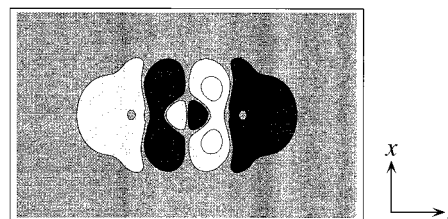


**Figure 8.** Calculated  $\gamma_{zzzz}$  value and plot of  $\gamma_{zzzz}$  density on the plane located at 2 au above the molecular plane of cation radical tetrathiapentalene (TTF<sup>•+</sup>). The B3LYP method using an extended (6-31G\*\*+d) basis sets is used. Contours are drawn at 10, 1, 0, -1, and -10 au.

This indicates that the contribution in the S-S-S region is enhanced by electron donation caused by the introduction of D(=NH<sub>2</sub>) groups into **2** and **5** positions (see Figure 1a). On the other hand, the contribution in the NH<sub>2</sub>-C-CH-C-CH-C-NH<sub>2</sub> region is shown to be small due to the cancellation of positive and negative contributions though the magnitudes of  $\gamma$  densities in that region are somewhat enhanced by NH<sub>2</sub> groups compared with those in the H-C-CH-C-CH-C-H region for TTP.

In contrast, for NO<sub>2</sub>-disubstituted TTP (see Figure 7b), the remarkable enhancements of  $\gamma$  densities are found to occur in the NO<sub>2</sub>-C-CH-C-CH-C-NO<sub>2</sub> region. Namely, the positive contribution in the S-S-S region is reduced and that in the NO<sub>2</sub>-C-CH-C-CH-C-NO<sub>2</sub> region is remarkably enhanced. Although the negative contribution is detected in the internal region of NO<sub>2</sub>-C-CH-C-CH-C-NO<sub>2</sub>, i.e., the C-CH-C-CH-C region, the large positive contribution caused by both ends of the NO<sub>2</sub> groups is found to make the total  $\gamma$  positive. This feature indicates that the contributions in the S-S-S and NO<sub>2</sub>-C-CH-C-CH-C-NO<sub>2</sub> regions are respectively reduced and enhanced owing to electron attraction caused by the introduction of A(=NO<sub>2</sub>) groups into **2** and **5** positions (see Figure 1a).

## 6. $\gamma$ and $\gamma$ Densities for TTF<sup>•+</sup>

**6.1.  $\gamma$  Density Analysis of TTF<sup>•+</sup>.** Figure 8 shows a plot of  $\gamma$  density and  $\gamma$  value for TTF<sup>•+</sup> calculated by B3LYP method

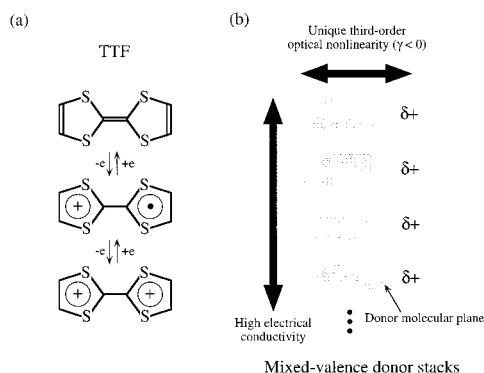


**Figure 9.** (a) Two-step redox reaction process for tetrathiapentalene (TTF). (b) A multiproperty aggregate model combining high electrical conductivity and unique third-order optical nonlinearity. The mixed-valence stack is composed of partially cationic donor molecules.

using 6-31G\*\*+d basis set.<sup>17</sup> The  $\gamma$  density distribution located at 2 au above the molecular plane is drawn since we confine our attention to the contribution of  $\pi$  electrons, which mainly contribute to the  $\gamma$ .

Judging from the contribution of SRIP shown in Figure 2d,  $\text{TTF}^{+\bullet}$  (Figure 3d) is expected to exhibit negative longitudinal  $\gamma$ . In fact, the  $\gamma$  value for  $\text{TTF}^{+\bullet}$  calculated by B3LYP/6-31G\*\*+d is found to be negative in sign. The contributions of  $\gamma$  density distributed on S atoms (2, 5, 7, and 10 (see Figure 3d) are found to be negative, while the contributions of  $\gamma$  density distributed on C atoms (3, 4, 1, 6, 8, and 9 (see Figure 3d) are found to be positive. Since the magnitudes of  $\gamma$  densities on S atoms are found to be much larger than those of  $\gamma$  densities on C atoms, the total  $\gamma$  becomes negative in sign.

**6.2. A Prediction of  $\gamma$  for Segregated Molecular Aggregates.** It has been well-known that some molecular crystals composed of  $\pi$ -molecular D and A molecules have considerably high electrical conductivity.<sup>18,24</sup> These materials form the field of "organic semiconductors". Particularly, tetracyano-*p*-quinodimethane (TCNQ) radical anion forms a large number of organic semiconductors with various cation molecules such as TTF. Many of these crystals have a 1:2 ratio of cation to TCNQ. It was found that the high electrical conductivity is closely related to the crystal structures composed of the segregated stacks of D and A molecules which are planar molecules packed face-to-face. The  $\pi$  overlap and charge transfer (CT) interaction between adjacent molecules in the stacking direction are found to be responsible for the electrical conductivity in the direction. In general, there are found to be three types of segregated molecular crystals: (A) ionic crystals in which complete CT occurs from D to A molecules, (B) neutral crystals in which no CT occurs due to Coulomb interactions, and (C) partially ionic, mixed-valence crystals in which incomplete CT occurs. It is well-known that the type C system tends to exhibit high electrical conductivity in the stacking direction, while the types A and B systems become a low-conductive or nonconductive aggregates.<sup>18</sup> We here particularly consider the type C system in relation to a possibility of multiproperty system combined with unique third-order nonlinearity and high electrical conductivity.

In the case of mixed-valence crystal (type C), the D stacks have partially positive charges due to incomplete CT from D to A molecules. In chemical picture, the cation radical state of donor molecule (the second redox state shown in Figure 9a) is considered to be partly generated in the mixed-valence crystal. The D molecules shown in Figure 9b are also considered to have partially positive charges, e.g.,  $\text{TTF}^{\delta+\bullet}$  ( $0 < \delta < 1$ ).

Judging from SRIP contributions of  $\text{TTF}^{+\bullet}$  shown in Figure 2d, these partially cationic radical states of D molecules tend to have large contribution of SRIP in the direction perpendicular to the stacking direction (see Figure 9b). If the  $\delta$  is nearly equal to 0.5 and the SRIP contribution is large enough to provide negative  $\gamma$ , there is a possibility of realizing a multiproperty aggregate system combined with high electrical conductivity and unique third-order optical nonlinearity, i.e., negative  $\gamma$ , in the direction perpendicular to the stacking direction.

## 7. Concluding Remarks

In this study, we theoretically presented a new class of third-order nonlinear optical systems involving S atoms and investigated the features of their  $\gamma$  by ab initio and DF calculations.

First, we analyzed  $\pi$ -electron contribution for TTP to the longitudinal  $\gamma$  by using  $\gamma$  density plot. It was found for TTP that the  $\pi$ -electrons in the S—S—S region mainly contribute to the longitudinal  $\gamma$  positively, while the  $\pi$ -electron contribution in the H—C—CH—C—CH—C—H region is small negative.

Secondly, we investigated the effects of the introduction of D(=NH<sub>2</sub>) and A(=NO<sub>2</sub>) groups into 2 and 5 positions of TTP on the longitudinal  $\gamma$ . Although the  $\gamma$  values for both systems, i.e., NH<sub>2</sub>- and NO<sub>2</sub>-disubstituted TTP, were found to be largely enhanced compared with that of TTP, there were found to be remarkable differences in the feature of spatial contributions to  $\gamma$ . Namely, the electron donating property of NH<sub>2</sub> group enhances the positive contribution in the S—S—S region, while the electron attracting property of NO<sub>2</sub> group reduces the contribution in the S—S—S region and enhance that in the NO<sub>2</sub>—C—CH—C—CH—C—NO<sub>2</sub> region. Judging from these results, the magnitude of contribution for  $\pi$ -electrons to the  $\gamma$  for disubstituted TTP is expected to be controlled by changing the electron donating and attracting properties for D and A groups.

Finally, as a rare molecule with negative  $\gamma$ , cation radical TTF was proposed based on our structure-property correlation rule using SRIP contribution. From the longitudinal  $\gamma$  and its density plot calculated by B3LYP calculation, the  $\gamma$  value and the contribution of  $\pi$ -electrons were found to be negative. This molecule is also well-known to be a good D molecule constructing high electrical conductive molecular aggregates, e.g., mixed-valence stacks composed of partially cationic radical states of D molecules. In such systems, the conduction electrons are considered to transfer in the stacking direction and the unique negative  $\gamma$  is also expected to be generated in the direction perpendicular to the stacking direction. This suggests a possibility of multiproperty systems combining high electrical conductivity and unique third-order optical nonlinearity ( $\gamma < 0$ ). At the next stage, band calculations involving the correlation between conduction electrons in the stacking direction and third-order hyperpolarization in the perpendicular direction to the stacking direction will be performed in order to confirm the prediction and suggestion presented in this study.

**Acknowledgment.** This work was supported by Grant-in-Aid for Scientific Research on Priority Areas (Grant 10149101) from Ministry of Education, Science, Sports and Culture, Japan, and a Grant from CASIO Science Promotion Foundation.

## References and Notes

- (1) Prasad, P. N.; Williams, D. J., *Introduction to Nonlinear Optical Effects in Molecules and Polymers*; Wiley: New York, 1990.
- (2) Nakano, M.; Yamaguchi, K. *Analysis of Nonlinear Optical Processes for Molecular Systems*; Trends in Chemical Physics 5; Research Trends: Trivandrum, India, 1997; pp 87–237.
- (3) Nakano, M.; Yamaguchi, K. *Chem. Phys. Lett.* **1993**, 206, 285.

- (4) Nakano, M.; Kiribayashi, S.; Yamada, S.; Shigemoto, I.; Yamaguchi, K. *Chem. Phys. Lett.* **1996**, 262, 66.
- (5) Bessi, S.; Mammi, M.; Garbuglio, C. *Nature* **1958**, 182, 247.
- (6) Cimiraglia, R.; Hofmann, H.-J. *J. Am. Chem. Soc.* **1991**, 113, 6449.
- (7) Shen, Q.; Hedberg, K. *J. Am. Chem. Soc.* **1974**, 96, 289.
- (8) Saebø, S.; Boggs, J. E.; Fan, K. *J. Phys. Chem.* **1992**, 96, 9268.
- (9) S-Larsen, J.; Erting, C.; Shim, I. *J. Am. Chem. Soc.* **1994**, 116, 11433.
- (10) Takane, S.; Sakai, S. *J. Mol. Struct. (Theochem.)* **1999**. In press.
- (11) Nakano, M.; Shigemoto, I.; Yamada, S.; Yamaguchi, K. *J. Chem. Phys.* **1995**, 103, 4175.
- (12) Shen, Y. R. *The Principles of Nonlinear Optics*; Academic: New York, 1984.
- (13) Nakano, M.; Yamaguchi, K. *Mol. Cryst. Liq. Cryst. A* **1994**, 255, 139.
- (14) Yamada, S.; Nakano, M.; Yamaguchi, K. *Chem. Phys. Lett.* **1997**, 276, 375.
- (15) Yamada, S.; Nakano, S.; Shigemoto, I.; Kiribayashi, S.; Yamaguchi, K. *Chem. Phys. Lett.* **1997**, 267, 438.
- (16) Nakano, M.; Yamada, S.; Yamaguchi, K. *Bull. Chem. Soc. Jpn.* **1998**, 71, 845.
- (17) Nakano, M.; Yamada, S.; Yamaguchi, K. Submitted for publication.
- (18) Torrance, J. B.; *Acc. Chem. Res.* **1979**, 12, 79.
- (19) Becke, A. D. *J. Chem. Phys.* **1993**, 98, 5648.
- (20) Frisch, M. J.; Trucks, G. W.; Head-Gordon, M.; Gill, P. M. W.; Wong, M. W.; Foresman, J. B.; Johnson, B. G.; Schlegel, H. B.; Robb, M. A.; Replogle, E. S.; Gomperts, R.; Andres, J. L.; Raghavachari, K.; Binkley, J. S.; Gonzalez, C.; Martin, R. L.; Fox, D. J.; Defrees, D. J.; Baker, J.; Stewart, J. J. P.; Pople, J. A. *Gaussian 94*, Revision B.1; Gaussian, Inc.: Pittsburgh, PA, 1995.
- (21) Calaminici, P.; Jug, K.; Köster, A. M. *J. Chem. Phys.* **1998**, 109, 7756.
- (22) Yamada, S.; Nakano, M.; Shigemoto, I.; Yamaguchi, K. *Chem. Phys. Lett.* **1996**, 254, 158.
- (23) de Melo, C. P.; Silbey, R. *J. Chem. Phys.* **1987**, 88, 2567.
- (24) Gutmann, F.; Lyons, J. E. *Organic Semiconductors*; Wiley: New York, 1967.